Heliyon 6 (2020) e04815

Contents lists available at ScienceDirect

Heliyon

journal homepage: www.cell.com/heliyon

Research article

Analysis of the distribution of microfractures and micropores within granitic rock using simultaneous polarization–fluorescence microscopy

Takashi Yuguchi [a,*], Akane Usami [a], Masayuki Ishibashi [b]

[a] Faculty of Science, Yamagata University, 1-4-12 Kojirakawa, Yamagata, 990-8560, Japan
[b] Japan Atomic Energy Agency, 1-64, Yamanouchi, Akiyo, Mizunami, Gifu, 509-6132, Japan

ARTICLE INFO

Keywords:
Earth sciences
Geology
Microfracture
Micropore
Microscopic void
Simultaneous polarization-fluorescence
Microscopy
Thin section
Toki granitic pluton

ABSTRACT

The analysis of the distribution of microfractures and micropores is important to accurately characterise mass transfer within a rock body. In this paper, a new 'simultaneous polarization–fluorescence microscopy' method is presented, which can be used to analyse the distribution of microscopic voids, including microfractures and micropores, in granitic rock. In this method, thin sections prepared with fluorescent dye are analysed under a polarizing microscope equipped with a fluorescent reflected light source. Using both the transmitted and the fluorescent light sources, both the distribution of microfractures and micropores, and petrographic characteristics (mineral occurrences) can be determined efficiently and simultaneously. The distribution of microfractures and micropores observed in images of granites obtained using simultaneous polarization–fluorescence microscopy is consistent with the distribution observed in backscattered electron images. The low magnification characterisation of the distribution of microscopic voids also provides targeting for subsequent studies including scanning electron microscopy under high magnification, chemical analysis, and image processing.

1. Introduction

The characterisation of mass transfer within granitic rock (e.g. pathway, rate, and direction) contributes to safety evaluations of the geological disposal of nuclear waste and the geological storage of oil and natural gas. Microfractures and micropores in minerals act as migration pathways for mass transfer through granitic rock (e.g. Ishibashi et al., 2014, 2016b; Yuguchi et al., 2019). Therefore, the characterisation of microfractures and micropores deduced from both of low- and high-resolution analyses is important to accurately evaluate mass transfer within a rock body. High-resolution analyses (e.g. SEM analysis) can provide the detailed characterisation of microfractures and micropores (e.g. measurement and parameterization), while lower-resolution analytical techniques are required to understand their distributions. In this respect, this study presents an analytical method for evaluating the distribution of microfractures and micropores based on simultaneous polarization–fluorescence microscopy as lower resolution analytical technique.

In a previous study dealing with the analysis of the distribution of microfractures and micropores, Takagi et al. (2008) described the distribution of open microfractures in granitic minerals, based on polarized light microscope (POM) and cathodoluminescence images. Li et al. (2017) presented a method of fracture characterisation in carbonate rock using Sony TA-1150 X-ray computed tomography (CT) imagery. Although the X-ray CT imagery can provide three-dimensional information about fractures within a rock sample (e.g. Johns et al., 1993; Ketcham et al., 2010; Cnudde and Boone, 2013). A combination of X-ray CT imagery with the ^{14}C-labelled-polymethylmethacrylate method can provide three-dimensional distributions of minerals and porosities in granitic rock at a high-resolution (e.g. Voutilainen et al., 2012; Mazurier et al., 2016). Method of confocal scanning laser microscopy also can characterise the three-dimensional fracture network in granite sample (e.g. Montoto et al., 1995; Menéndez et al., 1999). However, their methods can be difficult to get access.

Ishibashi et al. (2016a) employed a fluorescence microscope equipped with a polarization system (Leica M205 FA). Based on this system, they obtained fluorescence microscopy (FLM; excitation wavelength: 450–490 nm, absorption wavelength: >500 nm) and POM images. The distribution of microfractures and micropores, and petrographic information were obtained by overlaying the FLM and POM images using digital image processing. Yuguchi et al. (2019) described the distribution and shapes of micropores within altered plagioclase based on

* Corresponding author.
E-mail address: takashi_yuguchi@sci.kj.yamagata-u.ac.jp (T. Yuguchi).

https://doi.org/10.1016/j.heliyon.2020.e04815
Received 5 February 2020; Received in revised form 27 February 2020; Accepted 25 August 2020

backscattered electron (BSE) images obtained using SEM. Although the method of Ishibashi et al. (2016a) is favourable for low magnification observations, real-time observations of both microfractures and petrographic information cannot be made because the FLM and POM images have to be captured separately and then overlain. Although SEM analysis, such as that reported by Yuguchi et al. (2019), can be used to observe the chemical variation of plagioclase and micropores with higher resolution, the distribution of micropores over a wide area cannot be evaluated. We therefore present a new easy-to-use 'simultaneous polarization–fluorescence microscopy (PFM)' method, which can be used to efficiently and simultaneously determine both the distribution of microfractures and micropores and petrographic characteristics in thin sections of rock samples. This paper presents the methods of the PFM technique, evaluates the technique and its application to granitic rock samples, and finally discusses the contribution of this method to the analysis of mass transfer.

2. Material and methods

The rock samples used to test the PFM method are from the Toki granite, central Japan, and were collected from the Mizunami Underground Research Laboratory. The laboratory consists of two vertical shafts (a main and a ventilation shaft) that are 500 m deep and range from 201 m above sea level (a.s.l., ground level) to an altitude of -299 m a.s.l.. (shaft bottom). Biotite chloritization (Yuguchi et al., 2015) and plagioclase alteration (Yuguchi et al., 2019) have been reported from the ventilation shaft at a depth of ~500 m (-299 m a.s.l.). The samples used in this study were collected from the deepest part of the ventilation shaft (-274 to -314 m a.s.l.). The petrography of the Toki granite at the sample site has been described in detail by Yuguchi et al. (2015, 2019). Many BSE images of the plagioclase and biotite minerals was collected to compare the distribution of microfractures and micropores in the PFM and BSE images.

The petrographic thin sections were produced by adhesion of the rock sample (about thickness of 0.03 mm) and glass slide (Figure 1). In this study, the adhesive included a fluorescent dye (bisphenol A) and water-insoluble with viscosity of 20,000–40,000 mPa·s. The adhesive material infiltrates microfractures and micropores in the sample, causing them to fluorescence under a fluorescent light. The water-insoluble adhesive prevents the decomposition of hydrous secondary minerals (e.g. clay). Thus, microfractures and micropores filled by the secondary mineralisation do not exhibit blue fluorescence in the PFM images.

The PFM apparatus consists of a polarizing microscope (Carl Zeiss Axio Lab. A1 POL) and a light source for fluorescence excitation (MeCan Adjustable lamp, fluorescence excitation light: 470 nm; Figure 1). The light emitted by the transmitted light source below passes through the polarizing filters and the thin section; simultaneously, the thin section is illuminated by the fluorescence excitation light source from the above (Figure 1). Light irradiation of the thin section leads to blue fluorescence of microfractures and micropores. The blue light passes through the upper polarizing filter where it combines with the transmitted polarized light to produce the PFM image. Therefore, the polarization and fluorescence systems used for simultaneous observations do not interfere with each other. This method can provide real-time observations of both microfractures and petrographic information.

The area (pixel area) of the minerals and microvoids were determined using Photoshop® image processing software. Image analysis revealing the areal fractions of the microvoids in the minerals were demonstrated with PFM images of biotite and plagioclase as an example (Figure 2). The biotite of Figure 3C-2 features microvoids along its cleavages; the altered plagioclase of Figure 4A-2 contains micropores. The biotite and plagioclase were clipped from the PFM images (Figure 2A-1 and B-1). Figure 2A-2 and B-2 show the binary images of the biotite and altered plagioclase. Black pixels consist of the target minerals and microvoids (1,430,151 pixels of Figure 2A-2, and 908,774 pixels of Figure 2B-2), while white pixels correspond to areas other than the target minerals.

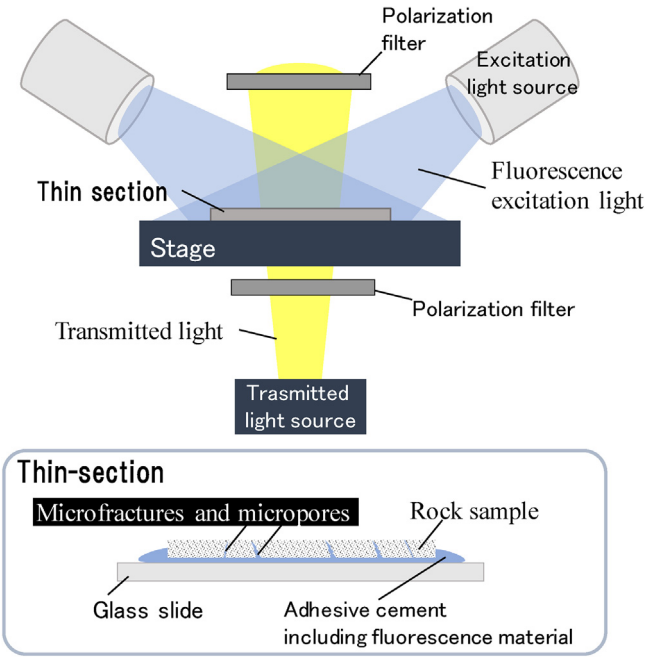

Figure 1. Schematic of the simultaneous polarization–fluorescence microscopy setup.

The black pixels in the binary image of Figure 2>A-3 correspond to the biotite area (1,192,377 pixels); those of Figure 2B-3 correspond to the plagioclase area (860,296 pixels). Thus, the areal fractions of the microvoids are 0.166, i.e. (1,430,151–1,192,377 pixels)/1,192,377 pixels in the biotite, and 0.053, i.e. (908,774–860,296) pixels/860,296 pixels in the altered plagioclase.

3. Results and discussion

Figure 3 shows POM and PFM images of the Toki granite. The PFM images of samples No. 12-2 (A-2), 9-8 (B-2), and 12-2' (C-2) show both the petrological characteristics and the distribution of blue fluorescent dye. The altered areas of plagioclase contain high-frequency, fluorescent blue dye with patchy shape. In unaltered areas, the dye occurs as low-frequency, long and linear shapes (Figure 3A-2 and B-2). The POM, PFM, and BSE images of altered plagioclase (sample 9-4) in Figure 4 show that the altered area irregularly branches out in multiple directions, indicating the infiltration channels of hydrothermal fluids (Yuguchi et al., 2019). The plagioclase also includes altered areas with large amounts of fluorescent dye observed in the PFM images and unaltered areas with small amounts of dye (Figure 4A-2 and B-2). The BSE images of the target plagioclase show that altered areas include columnar and granular micropores smaller than 15 μm (Figure 4C). Altered areas contain more micropores than the unaltered areas. Therefore, the blue fluorescence dye observed in the PFM images of plagioclase corresponds to the distribution of micropores. The area (pixel area) of the microvoids in the altered plagioclase was determined by image analysis (Figure 2). The corresponding volume was estimated by simply assuming area–volume equivalence (Yuguchi and Nishiyama, 2008), and the volume fraction of the microvoids was evaluated to be about 0.053.

Microfractures in quartz appear as connected lineations of fluorescent dye (Figure 3A-2 and C-2). The brightness and width of these lineations can be used to estimate the aperture size of the microfractures. K-feldspar has turbid areas, in which large amounts of fluorescent dye occur as patches in the PFM images (Figure 3A-2 and B-2). The turbid areas were caused by hydrothermal alteration and are associated with the distribution of micropores (Waldron et al., 1994). Therefore, the fluorescent dye within K-feldspar corresponds to the distribution of micropores. In the

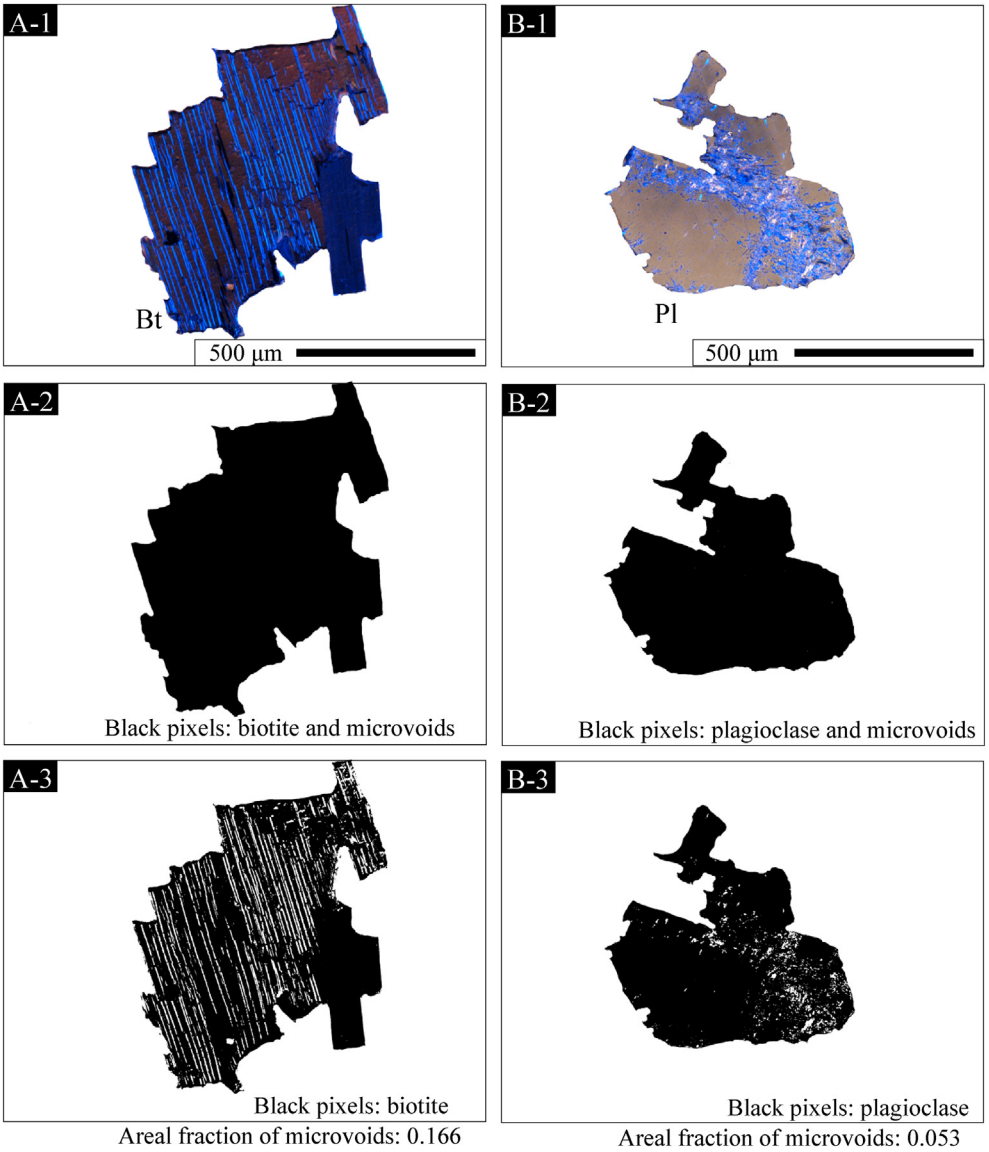

Figure 2. Image analysis revealing the volume (areal) ratios of the alteration minerals obtained using image processing software, with PFM images of plagioclase and biotite as an example.

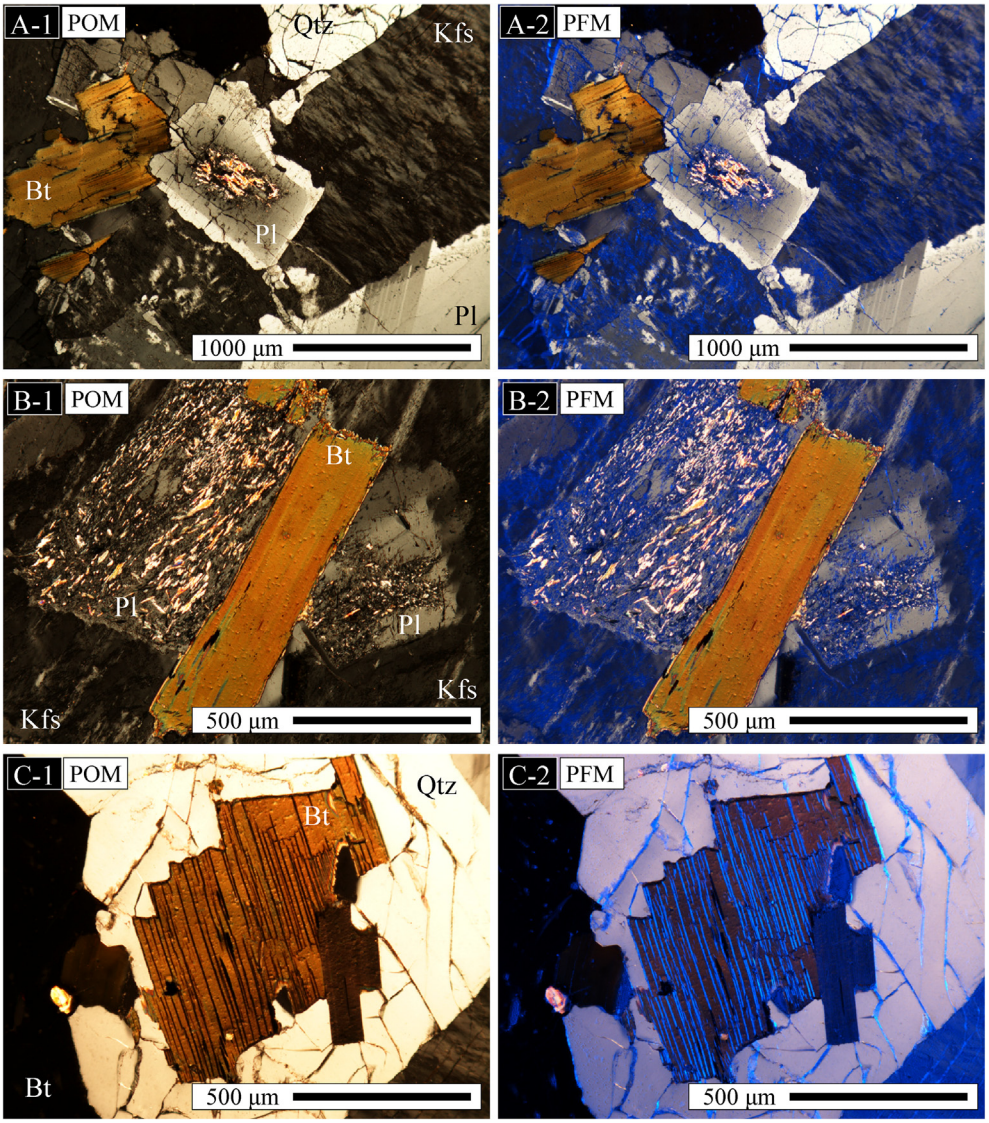

Figure 3. Polarization microscopy images (POM: A-1, B-1 and C-1) and simultaneous polarization–fluorescence microscopy images (PFM: A-2, B-2 and C-2). A: sample No. 12-2, B: sample No. 9-8 and C: sample No. 12-2'.

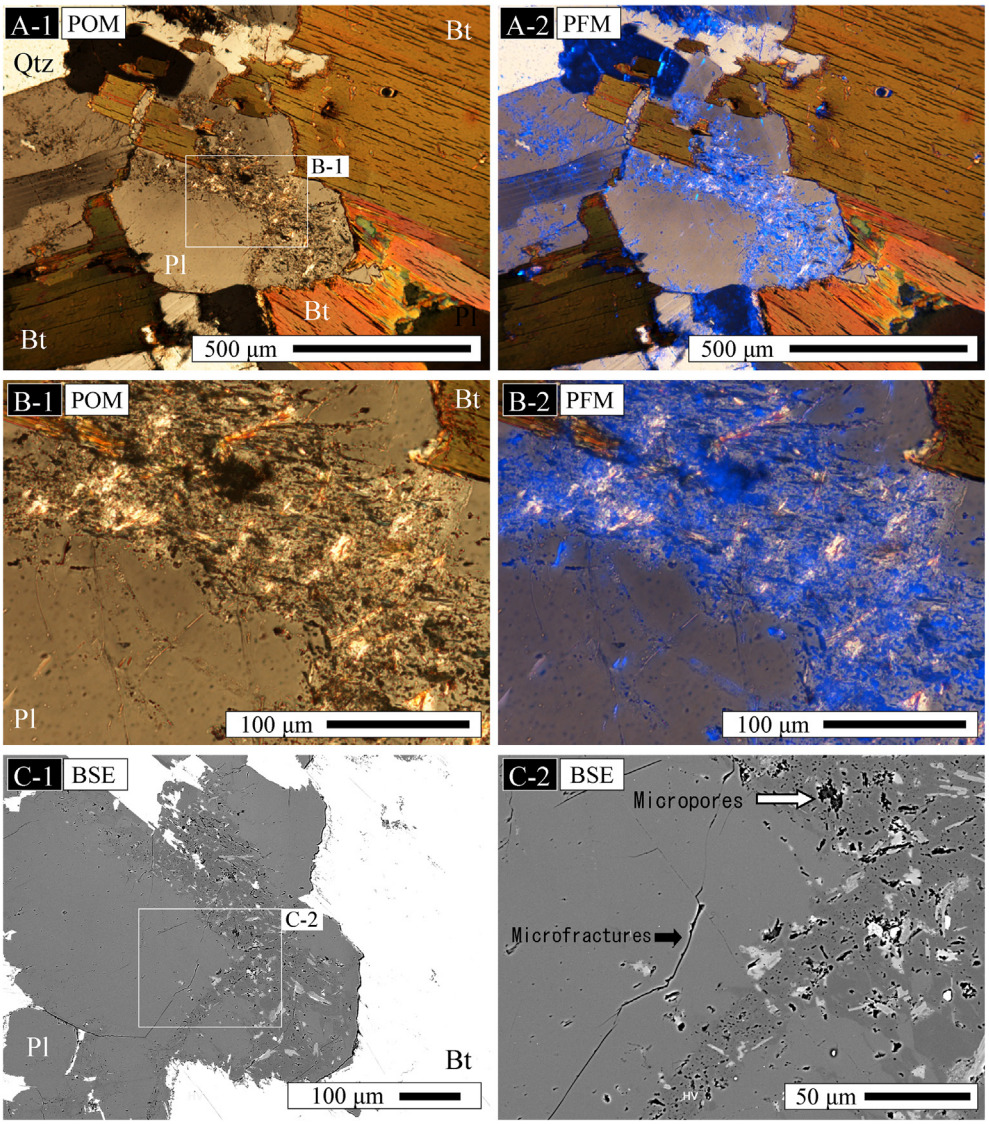

Figure 4. Polarization microscopy (POM) images (A-1 and B-1), simultaneous polarization–fluorescence microscopy (PFM) images (A-2 and B-2), and backscattered electron (BSE) images (C-1 and C-2), showing the altered plagioclase with channel structures resulting from hydrothermal fluid infiltration (sample No. 9-4).

PFM images, the biotite cleavage is fluorescent (Figure 3A, B and C). The biotite cleavage shown in Figure 3C is brighter and wider than other biotite cleavages, indicating wider apertures. According to image analysis, the volume fraction of the microvoids in biotite is about 0.166 (Figure 2). Therefore, micropores in biotite act as pathways for high-efficiency mass transfer.

Our results indicate that the blue fluorescence observed in PFM images reflects the distribution of voids (microfractures, micropores, and cleavage). Polarization–fluorescence microscopy is a powerful tool to simultaneously determine both the distribution of microscopic voids and mineral occurrences. It enhances the technique of Ishibashi et al. (2016a) by allowing the FLM and POM image data to be collected simultaneously. Detailed characterisation of the distribution of microscopic voids under low magnifications allows target points to be identified for analyses with high-resolution techniques. Thus, PFM contributes to a workflow from low-to high-magnification analyses including scanning electron microscopy, chemical analysis, and image processing that can be used to evaluate the distribution of mass transfer pathways within granitic rocks (Figure 5).

4. Conclusions

Simultaneous polarization–fluorescence microscopy (PFM) can be used to identify both the distribution of microscopic voids (e.g. microfractures, micropores, and cleavage) and the petrographic characteristics in thin sections of rock samples. The PFM apparatus consists of a polarizing microscope equipped with a light source for fluorescence excitation. White light emitted by the lower light source is transmitted through the polarizing filters and the thin section. Simultaneously, the thin section surface is excited by the light emitted from the fluorescent light source located above the sample. The polarized and fluorescent light systems do not interfere with each other during observation. Blue fluorescence in the PFM images reflects the distribution of microscopic voids. In the examined granites, the blue fluorescent dye within altered plagioclase corresponded to the distribution of micropores, thereby demonstrating that PFM can provide real-time observations of both microfractures and petrographic information. The detailed characterisation of the distribution of microscopic voids under low magnification contributes to the subsequent higher resolution studies because it can

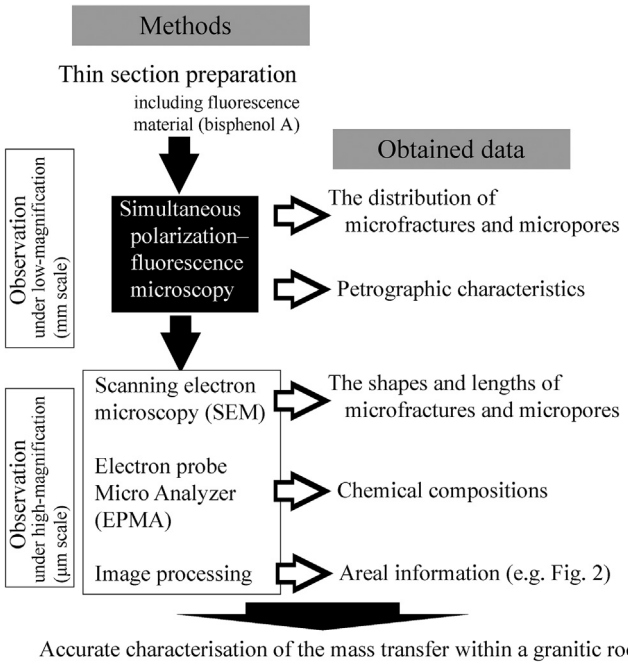

Figure 5. Flowchart the analyses used to accurately characterize mass transfer within granitic rock.

help to target the points for further analysis. Therefore, PFM is a useful method that can complement high magnification used in the evaluation of mass transfer pathways within granitic rocks. Our methodology is new in this field, and its validity and usefulness should be further evaluated in other granites and other lithologies for which an understanding of mass transfer pathways is important.

Declarations

Author contribution statement

T. Yuguchi: Conceived and designed the experiments; Performed the experiments; Analyzed and interpreted the data; Contributed reagents, materials, analysis tools or data; Wrote the paper.

A. Usami: Performed the experiments; Analyzed and interpreted the data.

M. Ishibashi: Contributed reagents, materials, analysis tools or data.

Funding statement

This work was supported by a Japan Society for the Promotion of Science (JSPS) KAKENHI for Young Scientists [grant number 16H06138] and a grant from the Ministry of Economy, Trade and Industry (METI), Japan to TY.

Competing interest statement

The authors declare no conflict of interest.

Additional information

No additional information is available for this paper.

Acknowledgements

Constructive reviews by four anonymous reviewers and Dr. Silas Michaelides (associated editor) were very helpful in revising the manuscript. The authors thank researchers of the Tono Geoscience Center, Japan Atomic Energy Agency (JAEA) for providing discussion and suggestions. The authors would like to thank Editage (www.editage.jp) for English language editing.

References

Cnudde, V., Boone, M.N., 2013. High-resolution X-ray computed tomography in geosciences: a review of the current technology and applications. Earth Sci. Rev. 123, 1–17.

Ishibashi, M., Ando, T., Sasao, E., Yuguchi, T., Nishimoto, S., Yoshida, H., 2014. Characterization of water conducting fracture and their long-term behavior in deep crystalline rock: a case study of the Toki granite. J. Japan Soc. Eng. Geol. 55, 156–165 (in Japanese with English abstract).

Ishibashi, M., Sasao, E., Hama, K., 2016a. Characteristics of micro transfer paths and diffusion phenomena in the matrix of deep crystalline rock. J. Nucl. Fuel Cycle Environ. 23, 121–129 (in Japanese with English abstract).

Ishibashi, M., Yoshida, H., Sasao, E., Yuguchi, T., 2016b. Long term behavior of hydrogeological structures associated with faulting: an example from the deep crystalline rock in the Mizunami URL, Central Japan. Eng. Geol. 208, 114–127.

Johns, R.A., Steude, J.S., Castanier, L.M., Roberts, P.V., 1993. Nondestructive measurements of fracture aperture in crystalline rock cores using X-ray computed tomography. J. Geophys. Res. 98, 1889–1900.

Ketcham, R.A., Slottke, D.T., Sharp, J.M., 2010. Three-dimensional measurement of fractures in heterogeneous materials using high-resolution X-ray computed tomography. Geosphere 6, 499–514.

Li, B., Tan, X., Wang, F., Lian, P., Gao, W., Li, Y., 2017. Fracture and vug characterization and carbonate rock type automatic classification using X-ray CT images. J. Petrol. Sci. Eng. 153, 88–96.

Mazurier, A., Sardini, P., Rossi, A.M., Graham, R.C., Hellmuth, K.H., Parneix, J.C., Siitari-Kauppi, M., Voutilainen, M., Caner, L., 2016. Development of a fracture network in crystalline rocks during weathering: study of Bishop Creek chronosequence using X-ray computed tomography and 14C-PMMA impregnation method. GSA Bullet. 128, 1423–1438.

Menéndez, B., David, C., Darot, M., 1999. A study of the crack network in thermally and mechanically cracked granite sample using confocal scanning laser microscopy. Phys. Chem. Earth Solid Earth Geodes. 24, 627–632.

Montoto, M., Martínez-Nistal, A., Rodríguez-Rey, A., Fernández-Meraya, N., Soriano, P., 1995. Microfractography of granitic rocks under confocal scanning laser microscopy. J. Microsc. 177, 138–149.

Takagi, H., Miwa, S., Yokomizo, Y., Nishijima, K., Enjyoji, M., Mizuno, T., Amano, K., 2008. Estimation of the paleostress field from 3-D orientation distribution of microcracks and their geothermal conditions in the Toki Granite, central Japan. J. Geol. Soc. Jpn. 114, 321–335 (in Japanese with English abstract).

Voutilainen, M., Siitari-Kauppi, M., Sardini, P., Lindberg, A., Timonen, J., 2012. Pore-space characterization of an altered tonalite by X-ray μCT and the 14C-labeled-polymethylmethacrylate method. J. Geophys. Res.: Solid Earth 117, B01201.

Waldron, K.A., Lee, M.R., Parsons, I., 1994. The microstructures of perthitic alkali feldspars revealed by hydrofluoric acid etching. Contrib. Mineral. Petrol. 116, 360–364.

Yuguchi, T., Nishiyama, T., 2008. The mechanism of myrmekite formation deduced from steady-diffusion modeling based on petrography: case study of the Okueyama granitic body, Kyushu, Japan. Lithos 106, 237–260.

Yuguchi, T., Sasao, E., Ishibashi, M., Nishiyama, T., 2015. Hydrothermal chloritization process from biotite in the Toki granite, Central Japan: temporal variation of chemical characteristics in hydrothermal fluid associated with the chloritization. Am. Mineral. 100, 1134–1152.

Yuguchi, T., Shoubuzawa, K., Ogita, Y., Yagi, K., Ishibashi, M., Sasao, E., Nishiyama, T., 2019. Role of micropores, mass transfer, and reaction rate in the hydrothermal alteration process of plagioclase in a granitic pluton. Am. Mineral. 104, 536–556.